Intervention Serology and Interaction Substitution: Modeling the Role of 'Shield Immunity' in Reducing COVID-19 Epidemic Spread

Joshua S. Weitz,[1,2,3,*] Stephen J. Beckett,[1] Ashley R. Coenen,[2] David Demory,[1] Marian Dominguez-Mirazo,[4,1] Jonathan Dushoff,[5,6] Chung-Yin Leung,[1,2] Guanlin Li,[4,2] Andreea Măgălie,[4,1] Sang Woo Park,[7] Rogelio Rodriguez-Gonzalez,[4,1] Shashwat Shivam,[8] and Conan Zhao[4,1]

[1] *School of Biological Sciences, Georgia Institute of Technology, Atlanta, GA, USA*
[2] *School of Physics, Georgia Institute of Technology, Atlanta, GA, USA*
[3] *Center for Microbial Dynamics and Infection, Georgia Institute of Technology, Atlanta, GA, USA*
[4] *Interdisciplinary Graduate Program in Quantitative Biosciences, Georgia Institute of Technology, Atlanta, GA, USA*
[5] *Department of Biology, McMaster University, Hamilton, ON, Canada*
[6] *DeGroote Institute for Infectious Disease Research, McMaster University, Hamilton, ON, Canada*
[7] *Department of Ecology and Evolutionary Biology, Princeton University, Princeton, NJ, USA*
[8] *School of Electrical and Computer Engineering, Georgia Institute of Technology, Atlanta, GA, USA*

(Dated: April 10, 2020)

The COVID-19 pandemic has precipitated a global crisis, with more than 1,430,000 confirmed cases and more than 85,000 confirmed deaths globally as of April 9, 2020 [1–4]. At present two central public health control strategies have emerged: mitigation and suppression (e.g, [5]). Both strategies focus on reducing new infections by reducing interactions (and both raise questions of sustainability and long-term tactics). Complementary to those approaches, here we develop and analyze an epidemiological intervention model that leverages serological tests [6, 7] to identify and deploy recovered individuals as focal points for sustaining safer interactions via interaction substitution, i.e., to develop what we term 'shield immunity' at the population scale. Recovered individuals, in the present context, represent those who have developed protective, antibodies to SARS-CoV-2 and are no longer shedding virus [8]. The objective of a shield immunity strategy is to help sustain the interactions necessary for the functioning of essential goods and services (including but not limited to tending to the elderly [9], hospital care, schools, and food supply) while decreasing the probability of transmission during such essential interactions. We show that a shield immunity approach may significantly reduce the length and reduce the overall burden of an outbreak, and can work synergistically with social distancing. The present model highlights the value of serological testing as part of intervention strategies, in addition to its well recognized roles in estimating prevalence [10, 11] and in the potential development of plasma-based therapies [12–15].

In the absence of reliable pharmaceutical interventions against SARS-CoV-2, multiple public health strategies are being deployed to slow the coronavirus pandemic [1, 5, 16]. These strategies can be broadly grouped into two approaches: mitigation; and suppression. Mitigation includes a combination of social distancing (including school and university closures), case testing, and symptomatic case isolation to reduce epidemic spread and burden on hospitals. Mitigation is intended to lessen an outbreak, however the level of disease may still overwhelm health services [5]. Instead, some jurisdictions have either pre-emptively or reactively adopted a combination of travel restrictions (shown to be effective in curtailing dispersion if implemented early enough [17, 18]) and suppression: imposing complete shut-downs of the bulk of non-essential services for extended periods (e.g., sheltering in place). Suppression has led to marked decreases in prevalence in the short term by combining case isolation, quarantine, use of separate facilities for treating COVID-19 patients, and large-scale viral testing to reduce transmission. Suppression also comes with significant costs, threatening social order and socio-economic health.

Here, we propose a complementary intervention approach that is intended to reduce transmission while lessening the costs of suppression and mitigation. The core idea is to leverage a mechanism of 'interaction substitution' by identifying and deploying recovered individuals who have protective antibodies to SARS-CoV-2. The intent is to develop population-level 'shield immunity' by amplifying the proportion of interactions with recovered individuals relative to those of individuals of unknown status (see Figure 1). Here, we assume that recovered individuals (i.e., virus-negative and antibody-positive) can safely interact with both susceptible and infectious individuals, in effect substituting interactions between susceptible and infectious individuals for interactions with a recovered individual. The intervention strategy is both local in scope and scales with outbreak size, given that the potential impact of shield immunity grows with a local outbreak. We recognize that our assumptions about safety for both recovered individuals and those they interact with is of vital importance. We return to this issue in discussing translational efforts

*Electronic address: jsweitz@gatech.edu; URL: `http://ecotheory.biology.gatech.edu`

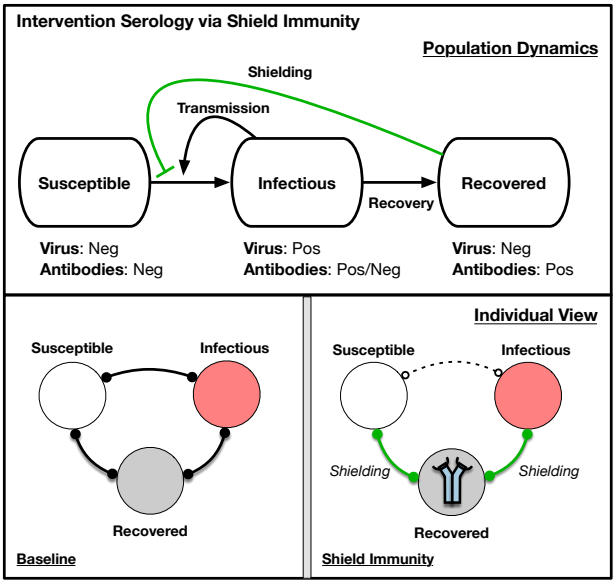

FIG. 1: Simplified schematic of intervention serology via shield immunity. (Top) Population dynamics of susceptible, infectious, and recovered in which recovered individuals reduce contact between susceptible and infectious individuals. Arrows denote flows between population level-compartments. (Bottom) Individual view of baseline scenario and shielding scenario, in which the identification, designation, and deployment of recovered individuals is critical to enabling S-R and I-R interactions to replace S-I interactions. Bonds denote interactions between individuals. In the Shield Immunity panel, the icon in the recovered individuals denotes the identification of individuals with protective antibodies, and hence the enhanced contribution of such individuals to shield immunity in contrast to the Baseline panel.

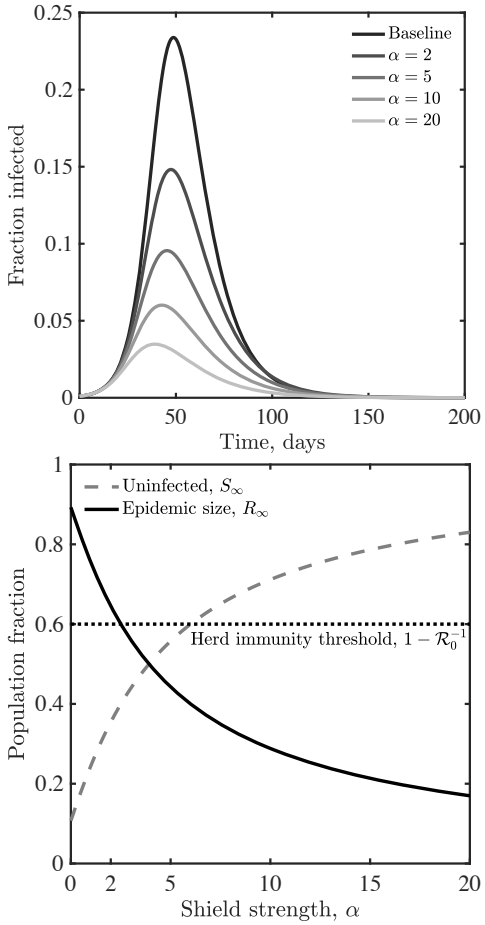

FIG. 2: Shield immunity dynamics in a SIR model. (Top) Infectious case dynamics with different levels of shielding, α. (Bottom) Final state of the system as a function of α. In both panels, $\beta = 0.25$ and $\gamma = 0.1$.

of shield immunity. To illustrate the concept of shield immunity, consider an epidemic model in which individuals tend to substitute their interactions with identified (or strategically located) recovered individuals. Hence, rather than mixing at random, we consider a relative preference of $1+\alpha$ that a given individual will interact with a recovered individual in what would otherwise be a potentially infectious interaction. This type of interaction substitution is equivalent to assuming an effective contact rate ratio of $1+\alpha$ for recovered individuals relative to the rest of the population. The dynamics of the fraction of susceptible S, infectious I, and recovered R individuals are:

$$\dot{S} = -\beta \frac{SI}{1+\alpha R} \quad (1)$$

$$\dot{I} = \beta \frac{SI}{1+\alpha R} - \gamma I \quad (2)$$

$$\dot{R} = \gamma I \quad (3)$$

such that when $\alpha = 0$ we recover the conventional SIR model. Note that the denominator of $1+\alpha R$ can be thought of as $S+I+R+\alpha R$. Given that $S+I+R=1$, this is equivalent to the term $1+\alpha R$. Figure 2 illustrates shield immunity impacts on an SIR epidemic with $\mathcal{R}_0 = 2.5$. In this SIR model, shield immunity reduces the epidemic peak and reduces epidemic duration. In effect, shielding acts as a negative feedback loop, i.e., given that the effective reproduction number is $\mathcal{R}_{eff}(t)/\mathcal{R}_0 = S(t)/(1+\alpha R(t))$. As a result, interaction substitution increases as recovered individuals increase in number and are identified. For example, in the case of $\alpha = 20$, the epidemic concludes with less than 20% infected in contrast to the final size of approximately 90% in the baseline scenario without shielding.

In order to explore the robustness of these findings, we examine 'flexible' and 'fixed' shielding as alternative interaction substitution mechanisms (see Methods). A flexible shielding mechanism represents enhanced *time-varying* interaction rates of recovered individuals by a factor of $(1+\alpha)$ relative to the interaction rate of other individuals, while keeping the total contact rate equal to that of the baseline (i.e., explicitly accounting for strict substitution of interaction). Likewise, a fixed shield-

ing mechanisms represents enhanced *time-fixed* interactions of recovered individuals by a factor of $(1+\alpha)$ relative to the baseline rate, while keeping the total contact rate equal to that of the baseline (i.e., again explicitly accounting for strict substitution of interactions). Extended Data Figure 1 shows that shielding is robust to these alternative scenarios, and indeed potentially even more effective. For example, in a fixed shielding mechanism with $\alpha = 3$, then recovered individuals sustain 4 times as many contacts relative to their pre-intervention baseline, ensuring the final outbreak concludes with less than 25% of the population having been infected compared to the expectation of $\approx$ 90% in the absence of shielding. We use our 'core' shielding model, described above as the basis for application to COVID-19, insofar as it represents the conservative benefits of shielding, while noting that detailed mixing and substitution models could lead to further variations of this model, e.g., in spatially explicit domains, on networks, etc. [19–22]. We revisit impacts of variation in shielding mechanisms on transmission and feasibility in the Discussion.

We next apply the concept of shield immunity to the epidemiological dynamics of the COVID-19 pandemic, ignoring births and other causes of deaths for simplicity. Consider a population of susceptible S, exposed E, infectious asymptomatically I_a, infectious symptomatically I_s, and recovered R who are free to move, without restrictions in a 'business as usual' scenario. A subset of symptomatic cases will require hospital care, which we further divide into subacute I_{hsub}, and critical/acute (i.e., requiring ICU intervention) I_{hcri} cases. We assume that a substantial fraction of critical cases will die. Age-stratified risk of hospitalization and acute cases are adapted from the Imperial College of London report [5]. The full model incorporating shield immunity (see SI for equations and details, and Extended Data Figure 2 for a schematic) differs from conventional SIR models with social distancing or case isolation interventions in a key way: the rate of transmission is reduced by a factor of $1/\left(N_{tot} + \alpha R_{shields}\right)$ where N_{tot} denotes the fraction of the population in the 'circulating baseline', and R_{shields} denotes the total number of recovered individuals between the ages of 20-60 (a subset of the total recovered population). In this model, we assume that all recovered individuals have immunity, but that only a subset are available to facilitate interaction substitutions. The model assumes that the circulating pool is not interacting with hospitalized patients, which must be incorporated into implementation scenarios with healthcare workers (HCW-s), who represent an intended target for shield immunity [23]). The baseline epidemiological parameters, age stratified risk, and population structure are listed in the SI (adapted from [5, 24–27]; see github for code and full implementation details).

We use the baseline epidemiological parameters and seed an outbreak with a single exposed individual until the outbreak reaches 0.1% total prevalence, e.g., 10,000 individuals infected out of a population of 10,000,000, at which point a shielding strategy is implemented. Outbreak scenarios differ in transmission rates, with $\mathcal{R}_0 = 1.57$ and 2.33 in the low and high scenarios, respectively. Early estimates of $\mathcal{R}_0$ from Wuhan are consistent with a 95% CI of between 2.1 and 4.5 [28], putting our high scenario on the conservative end of estimated ranges. However, the $\mathcal{R}_0$ of the high scenario we examine here is consistent with the range of 2.0 to 2.6 considered by the Imperial College London group [5], and with the median of $\mathcal{R}_{eff} = 2.38$ (95% CI: 2.04-2.77) as estimated via stochastic model fits to outbreak data in China that accounts for undocumented transmission [26]. Moreover, control measures reduce transmission, and our low scenario is consistent with estimates of $\mathcal{R}_{eff} = 1.36$ (95% CI: 1.14-1.63) in China from Jan. 24 to Feb. 3 after travel restrictions and other control measures were imposed. Figure 3 shows the results of comparing interventions to the baseline case. As in the simple SIR model, shielding (on its own) could potentially decrease epidemic burden across multiple metrics, decreasing both the total impact and shortening the peak event. In a population of size 10,000,000 for the high scenario, the final epidemic predictions are 71,000 deaths in the baseline case vs. 58,000 deaths given intermediate shielding ($\alpha = 2$), and 20,000 deaths given enhanced shielding ($\alpha = 20$). In a population of size 10,000,000 for the low scenario, the final epidemic predictions are 50,000 deaths in the baseline case vs. 34,000 deaths given intermediate shielding, and 8,300 deaths given enhanced shielding. The majority of deaths are in those ages 60 and above, despite the lower fraction of individuals in those ranges (see Figure 3), consistent with estimates in related COVID-19 models [5, 25, 26] and from outbreaks in Italy and China [29]. Note that our simulation results consider impacts based on shielding alone; whereas ongoing restrictions via social distancing and shelter in place orders will reduce interaction rates (a point we revisit later). The effectiveness of shielding depends on the product of the number of potential shields identified and their effective substitutability, i.e, αR, combining identification of and interaction rate by shields.

The population-scale impacts of shielding depends on multiple factors, including demographic distributions, the fraction of asymptomatic transmission ([24, 26]), and the duration of immunity. The SI treats each of these items at length. First, we find that populations with a strongly right-shifted demographic distribution will receive more potential benefits from shielding. Even though there are fewer recovered individuals between the ages of 20-60 to draw from (in a relative sense), the impact of shield immunity is greater. We find that the relative reduction in deaths via shield immunity is proportional to the relative differences in the fraction of population over 60 (e.g., see SI for details on US-state level analysis, similar results hold for countries like Italy where more than 23% of the population is older than 65 and nearly 30% is older than 60; Extended Data Figures 3). Second, shield immunity is robust to vari-

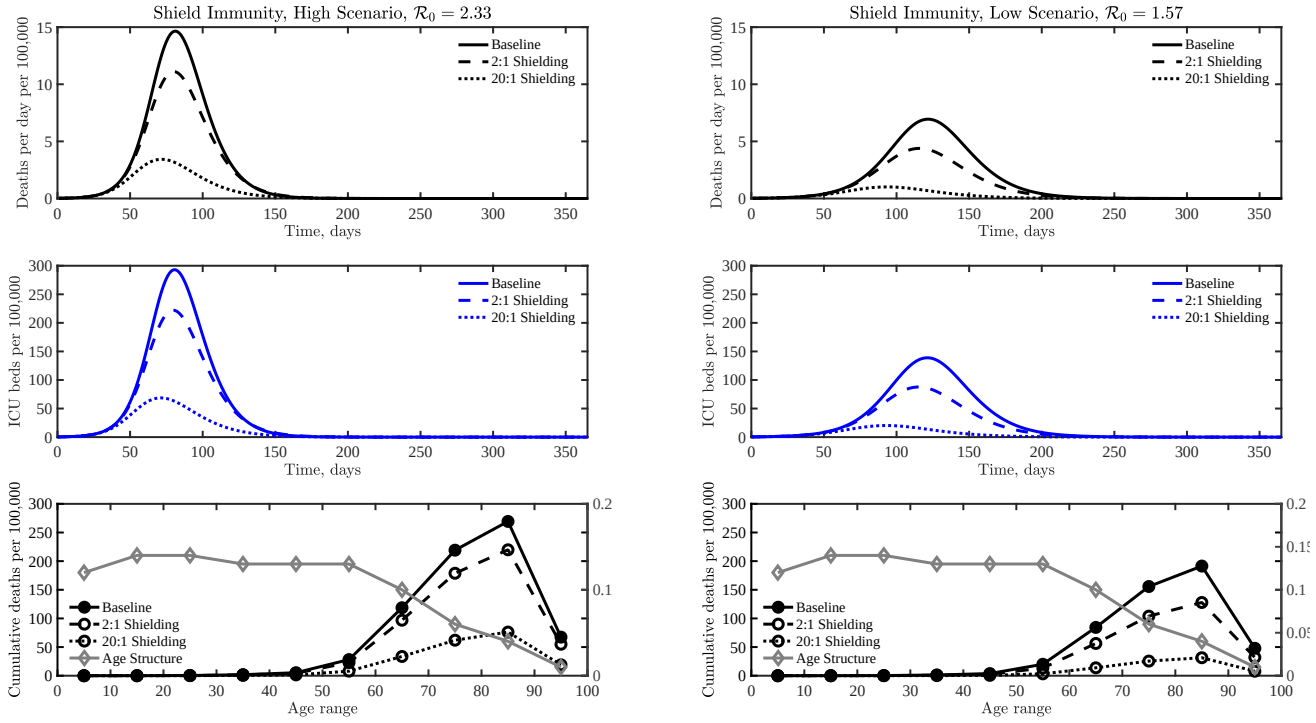

FIG. 3: COVID-19 dynamics in a baseline case without interventions compared to two shield immunity scenarios, $\alpha = 2$ and $\alpha = 20$, including deaths, ICU beds needed, and age distribution of fatalities. See the SI for more details on alternative scenarios, high (left) and low (right).

ation in asymptomatic infection probabilities, improving outcomes in models with varying baseline levels of asymptomatic transmission (see Extended Data Figures 4-6). In addition, the present model results assumes that immunity has relatively fast onset and is permanent in duration. Clinical work in Zhejiang University, China, suggests that seroconversion of total antibody (Ab), IgM and IgG antibodies developed with a median period of 15, 18, and 20 days post exposure, respectively (albeit for symptomatic patients in a hospital; similar data for seroconversion of asymptomatic individuals was not included [30]). In the SI we show that impacts of shield immunity is robust insofar as the duration of immunity is 4 months or longer (Extended Data Figures 7-8); we note that distinct control measures that extend the epidemic would likely impact effectiveness of shield immunity. For context, the titer of protective antibodies in individuals infected with related betacoronaviruses (causing mild/moderate symptoms) reduced over a one year period such that re-exposure can lead to re-infection [31], in contrast to evidence of multi-year immunity for individuals recovered from SARS [32]. In addition, we emphasize that the accuracy of serological tests is key. The benefits of shield immunity can be undermined if recovered individuals can be reinfected (even with little danger to them), or potentially misidentified, leading to interaction substitution with individuals that could infect others (a risk reduced by combining serology with PCR). Thus far we have focused on the impacts of shield immunity as a singular strategy, yet in practice, multiple interventions will be used in parallel. Hence, we evaluated the synergistic potential of utilizing shield immunity in combination with social distancing. Social distancing is modeled as a reduction in the transmission rates sustained over the post-intervention period. As is apparent in Figure 4, shielding can augment social distancing, particularly when social distancing is relatively ineffective. For example, contour lines of reduction in total fatalities suggest that a combination of 10% reduction in transmission with $\alpha = 20$ is equivalent to a nearly 50% reduction in transmission in the absence of shield immunity. However, there is a trade-off. Because social distancing reduces contacts and transmission, there are fewer recovered individuals when β is reduced by 50%. Nonetheless benefits of shielding accrue at all levels of social distancing. Social distancing and shield immunity may work in combination to improve outcomes in terms of expected hospitalization burden, again suggesting a role for shield immunity in reducing transmission and reducing the negative impacts of suppression-level social distancing policies. Finally, we note that targeted shield immunity may also enhance population outcomes by focusing the effort of recovered

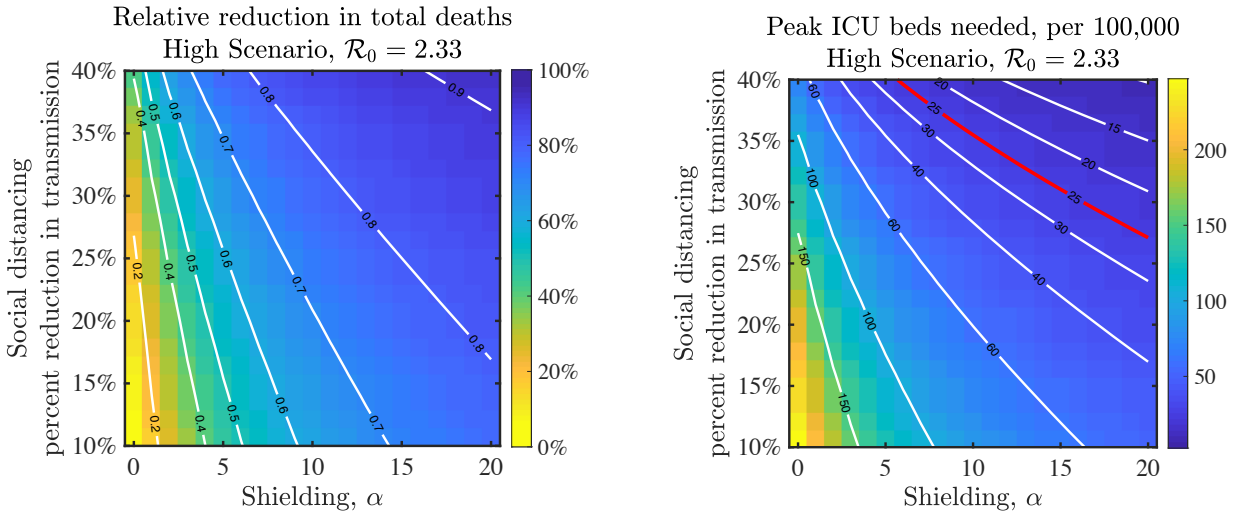

FIG. 4: Impacts of combined interventions of shielding and social distancing in the high scenario. (Left) Fractional reduction in deaths compared to baseline; (Right) Peak level of ICU beds needed on a given day during the epidemic; the red line denotes 25 ICU beds per 100,000 individuals as a demarcation point for surge capacity.

individuals in subsets of the population. In the SI, we show heuristic solutions to an optimization formulation of targeted (i.e., age-specific) shield immunity in this model. In effect, by preferentially targeting older individuals, it is possible to further reduce cumulative deaths by $\approx 30\%$ (see Extended Data Figures 9-10). Serological testing is needed now, at scale, for many reasons. Here, we have shown a rationale for serological testing as a means to facilitate interventions beyond those of mitigation and suppression. Identifying and deploying recovered individuals could represent more than just a metric of the state of the COVID-19 epidemic, e.g., to better measure prevalence and the 'denominator', but an opportunity to slow transmission by developing population-level shield immunity. Yet, logistical and social challenges must be addressed to implement shield immunity in practice.

First, accurate and rapid serological tests are needed at scale, including targeted surveys to identify essential workers and via population-level surveys. We recognize that serological test features would impact effective deployment. In evaluating the suitability of test features, high specificity is critical, so that people who are susceptible are not mistakenly identified as recovered (false positives). As of April 9, 2020, Cellex Inc. has the only FDA approved SARS-CoV-2 antibody test, with reported 96% specificity and 94% sensitivity [33]. Notably, there were no reported false positives out of 250 cases when combining IgG and IgM (at the cost of decreased sensitivity). In practice, the positive predictive value will vary with prevalence, suggesting that deployment may be more effective amongst groups that likely have elevated rates of current or past infection (whether because of outbreak scope, work setting, or other factors). The joint exploration of shield immunity with test characteristics warrants further exploration.

Second, the potential scale of shield immunity depends on both the intrinsic epidemic dynamics, driving the number of recovered individuals able to provide shield immunity, and also on the ability to identify and deploy them (e.g., via the shielding parameter α). Hence, as serological tests become widely available and (hopefully) improve in specificity, new questions will be raised with respect to test prioritization and action-taking for those who test positive for protective antibodies. Public health authorities and governmental agencies should consider how to prioritize those in critical roles, those with experience in disaster response, as well as prior individuals who have tested positive for COVID-19 (and could then return for both serology-based and viral shedding assays). Positive confirmation of immunity and cessation of viral shedding could help identify and deploy a substantial fraction of individuals as part of a shield immunity strategy, with the greatest concentration likely co-located with areas in greatest need of intervention. A national (or global) strategy could consider the deployment of critical response workers with protective antibodies to help control new outbreaks (see [34] for a related proposal in efforts to control the Ebola virus disease outbreak).

Third, we recognize there are significant challenges to developing and implementing interventions that aim to develop population-wide shield immunity. Nonetheless, the magnitude of the current public health and economic crisis demands large-scale action (e.g., [35, 36]). The efficacy of a shield immunity strategy depends on many other factors, including demographics and interaction context. Beyond the near-term, the duration of immune memory is also relevant in projecting to a multi-year post-pandemic framework where demographic dynamics and strain evolution are increasingly relevant [37, 38].

Hence, a serological testing initiative (with repeated testing over time) could benefit intervention efforts while also providing critical information on seroconversion and the risk of reinfection to recovered individuals.

Finally, it will be critical to understand how shield immunity is modulated by spatial and network structure. In a network, well-connected individuals have a disproportionate effect on the spread of disease [20]. Network structure represents an opportunity to position immune shields at focal points of 'essential' services, and even to prioritize the focus of population-scale serological prevalence assays based on the connectivity of targeted individuals. Indeed, in the present analysis we assumed that interactions with recovered individuals occurred at a rate $(1+\alpha)$ higher than with other individuals, enabling population-scale shield immunity to emerge well before herd immunity. However, there are multiple interaction mechanisms that could yield such interaction substitution, including both 'flexible' and 'fixed' shielding mechanisms that take different approaches to the extent to which recovered alone, or all individuals, modulate their contact rates. As shown in Extended Data Figure 1, these mechanisms have the potential to enhance the impact of shielding at lower levels of α, Further studies are needed to explore how these mechanisms could guide efforts to re-wire networked interactions to minimize transmission while also alleviating impacts of social distancing by (partially) restoring network connectivity.

Although the number of laboratory confirmed cases of COVID-19 is both staggering and growing, the actual number of infections is higher – likely far higher; for example in China, 80% of transmission of new cases were from undocumented infections [26] and there is significant uncertainty with respect to case ascertainment [39]. Asymptomatic transmission may paradoxically provide a greater pool of recovered individuals to develop shield immunity at scale. We contend that it is time for collective action to ascertain more information on outbreak size and to consider strategic use of serology as the basis for integrative public health interventions to control the pandemic spread of COVID-19.

1 Fauci, A. S., Lane, H. C. & Redfield, R. R. Covid-19 – navigating the uncharted. *New England Journal of Medicine* (2020). URL https://doi.org/10.1056/NEJMe2002387.

2 Li, Q. *et al.* Early transmission dynamics in Wuhan, China, of novel Coronavirus-infected pneumonia. *New England Journal of Medicine* **382**, 1199–1207 (2020). URL https://doi.org/10.1056/NEJMoa2001316.

3 Zhou, P. *et al.* A pneumonia outbreak associated with a new coronavirus of probable bat origin. *Nature* 270–273 (2020).

4 World Health Organization: Coronavirus disease 2019 (COVID-19) Situation Report - 70 (2020). URL https://www.who.int/docs/default-source/coronaviruse/situation-reports/20200409-sitrep-80-covid-19.pdf?sfvrsn=1b685d64_2.

5 Ferguson, N. *et al.* Impact of non-pharmaceutical interventions (npis) to reduce COVID19 mortality and healthcare demand (2020). URL https://www.imperial.ac.uk/media/imperial-college/medicine/sph/ide/gida-fellowships/Imperial-College-{COVID19}-NPI-modelling-16-03-2020.pdf.

6 Amanat, F. *et al.* A serological assay to detect SARS-CoV-2 seroconversion in humans. *medRxiv* (2020). URL https://www.medrxiv.org/content/early/2020/03/18/2020.03.17.20037713.

7 Okba, N. *et al.* SARS-CoV-2 specific antibody responses in COVID-19 patients. *medRxiv* (2020). URL https://www.medrxiv.org/content/early/2020/03/20/2020.03.18.20038059.

8 Zhao, J. *et al.* Antibody responses to SARS-CoV-2 in patients of novel coronavirus disease 2019. *medRxiv* (2020). URL https://www.medrxiv.org/content/early/2020/03/02/2020.03.02.20030189.

9 McMichael, T. M. *et al.* Epidemiology of Covid-19 in a long-term care facility in king county, washington. *New England Journal of Medicine* (2020). URL https://doi.org/10.1056/NEJMoa2005412.

10 Lourenco, J. *et al.* Fundamental principles of epidemic spread highlight the immediate need for large-scale serological surveys to assess the stage of the SARS-CoV-2 epidemic. *medRxiv* (2020). URL https://www.medrxiv.org/content/early/2020/03/26/2020.03.24.20042291.

11 Lipsitch, M., Swerdlow, D. L. & Finelli, L. Defining the epidemiology of Covid-19 – studies needed. *New England Journal of Medicine* **382**, 1194–1196 (2020). URL https://doi.org/10.1056/NEJMp2002125.

12 Chen, L., Xiong, J., Bao, L. & Shi, Y. Convalescent plasma as a potential therapy for COVID-19. *The Lancet Infectious Diseases* (2020).

13 Duan, K. *et al.* The feasibility of convalescent plasma therapy in severe COVID-19 patients: a pilot study. *medRxiv* (2020). URL https://www.medrxiv.org/content/early/2020/03/23/2020.03.16.20036145.

14 Roback, J. D. & Guarner, J. Convalescent plasma to treat COVID-19: Possibilities and challenges. *JAMA* (2020). URL https://doi.org/10.1001/jama.2020.4940.

15 National COVID-19 Convalescent Plasma Project. URL https://ccpp19.org/.

16 Hennekens, C. H., George, S., Adirim, T. A., Johnson, H. & Maki, D. G. The emerging pandemic of coronavirus: The urgent need for public health leadership. *The American Journal of Medicine* (2020). URL http://www.sciencedirect.com/science/article/pii/S0002934320302072.

17 Chinazzi, M. *et al.* The effect of travel restrictions on the spread of the 2019 novel coronavirus (COVID-19) outbreak. *Science* (2020). URL https://science.sciencemag.org/content/early/2020/03/05/science.aba9757.

18 Kraemer, M. U. G. *et al.* The effect of human mobility and control measures on the COVID-19 epidemic in china. *Science* (2020). URL https://science.sciencemag.org/content/early/2020/03/25/science.abb4218.

19 Watts, D. J., Muhamad, R., Medina, D. C. & Dodds, P. S. Multiscale, resurgent epidemics in a hierarchical metapopulation model. *Proceedings of the National Academy of Sciences* **102**, 11157–11162 (2005).

20 Bansal, S., Grenfell, B. T. & Meyers, L. A. When individual behaviour matters: homogeneous and network models in epidemiology. *Journal of the Royal Society Interface* **4**, 879–891 (2007).

21 Balcan, D. *et al.* Multiscale mobility networks and the spatial spreading of infectious diseases. *Proceedings of the National Academy of Sciences* **106**, 21484–21489 (2009).

22 Colizza, V., Barrat, A., Barthélemy, M. & Vespignani, A. The role of the airline transportation network in the prediction and predictability of global epidemics. *Proceedings of the National Academy of Sciences* **103**, 2015–2020 (2006).

23 Klompas, M. Coronavirus Disease 2019 (COVID-19): Protecting Hospitals From the Invisible. *Annals of Internal Medicine* (2020). URL `https://doi.org/10.7326/M20-0751`.

24 Park, S. W., Cornforth, D. M., Dushoff, J. & Weitz, J. S. The time scale of asymptomatic transmission affects estimates of epidemic potential in the COVID-19 outbreak. *medRxiv* (2020). URL `https://www.medrxiv.org/content/10.1101/2020.03.09.20033514v1`.

25 Wu, J. T., Leung, K. & Leung, G. M. Nowcasting and forecasting the potential domestic and international spread of the 2019-nCoV outbreak originating in Wuhan, China: a modelling study. *The Lancet* **395**, 689–697 (2020).

26 Li, R. *et al.* Substantial undocumented infection facilitates the rapid dissemination of novel coronavirus (SARS-CoV2). *Science* (2020). URL `https://science.sciencemag.org/content/early/2020/03/13/science.abb3221`.

27 Wu, J., Leung, K., Bushman, M. *et al.* Estimating clinical severity of COVID-19 from the transmission dynamics in Wuhan, China. *Nature Medicine* (2020). URL `https://doi.org/10.1038/s41591-020-0822-7`.

28 Park, S. W. *et al.* Reconciling early-outbreak estimates of the basic reproductive number and its uncertainty: framework and applications to the novel coronavirus (SARS-CoV-2) outbreak. *medRxiv* (2020). URL `https://www.medrxiv.org/content/10.1101/2020.01.30.20019877v4.full.pdf`.

29 Onder, G., Rezza, G. & Brusaferro, S. Case-fatality rate and characteristics of patients dying in relation to COVID-19 in Italy. *JAMA* (2020). URL `https://doi.org/10.1001/jama.2020.4683`.

30 Lou, B. *et al.* Serology characteristics of SARS-CoV-2 infection since the exposure and post symptoms onset. *medRxiv* (2020). URL `https://www.medrxiv.org/content/early/2020/03/27/2020.03.23.20041707`.

31 Callow, K., Parry, H., Sergeant, M. & Tyrrell, D. The time course of the immune response to experimental coronavirus infection of man. *Epidemiology & Infection* **105**, 435–446 (1990).

32 Chan, K.-H. *et al.* Cross-reactive antibodies in convalescent SARS patients' sera against the emerging novel human coronavirus EMC (2012) by both immunofluorescent and neutralizing antibody tests. *Journal of Infection* **67**, 130–140 (2013).

33 Cellex Inc Emergency Use Authorization. URL `https://www.fda.gov/media/136625/download`.

34 Bellan, S. E., Pulliam, J. R., Dushoff, J. & Meyers, L. A. Ebola control: effect of asymptomatic infection and acquired immunity. *The Lancet* **384**, 1499–1500 (2014).

35 Emanuel, E. J. We can safely restart the economy in June. Here's how. *The New York Times* (2020). URL `https://www.nytimes.com/2020/03/28/opinion/coronavirus-economy.html`.

36 Gottlieb, S., Rivers, C., McClellan, M., Silvis, L. & Watson, C. National coronavirus response: A road map to reopening. *American Enterprise Institute* (2020). URL `https://www.aei.org/research-products/report/national-coronavirus-response-a-road-map-to-reopening/`.

37 Hadfield, J. *et al.* Nextstrain: real-time tracking of pathogen evolution. *Bioinformatics* **34**, 4121–4123 (2018).

38 Kissler, S. M., Tedijanto, C., Goldstein, E., Grad, Y. H. & Lipsitch, M. Projecting the transmission dynamics of SARS-CoV-2 through the post-pandemic period. *medRxiv* (2020). URL `https://www.medrxiv.org/content/early/2020/03/06/2020.03.04.20031112`.

39 Flaxman, S. *et al.* Estimating the number of infections and the impact of nonpharmaceutical interventions on COVID-19 in 11 European countries (2020). URL `https://www.imperial.ac.uk/media/imperial-college/medicine/sph/ide/gida-fellowships/Imperial-College-COVID19-Europe-estimates-and-NPI-impact-30-pdf`.

Methods

Intervention Serology and Interaction Substitution: Modeling the Role of 'Shield Immunity' in Reducing COVID-19 Epidemic Spread

Shielding Mechanisms

In this section, we analyze alternative shielding mechanisms as extensions to the SIR model presented in the main text.

Force of infection: Consider the force of infection to be the contact rate of susceptible individuals multiplied by the probability that the interactions are with an infectious person multiplied by a probability that the event leads to an infection. Let c_S, c_I, c_R equal the contact rate of S, I, and R individuals respectively. Hence the force of infection should be proportional to:

$$c_S \left(\frac{c_I I}{c_S S + c_I I + c_R R} \right) \tag{1}$$

in which the weighted average of contacts is $c_0 = c_S S + c_I I + c_R R$. When $c_s = c_I = c_0$ and $c_R = c_0(1+\alpha)$ the force of infection is proportional to:

$$c_0 \left(\frac{I}{1+\alpha R} \right). \tag{2}$$

This is the basis for the core shielding model presented in the main text. We consider a 'flexible' and 'fixed' shielding mechanisms that keeps the weighted average constant throughout the dynamics.

Flexible shielding: In a flexible shielding mechanism, recovered individuals have $(1+\alpha)$ greater contact rates than do susceptible or infectious individuals. Denoting c_B as the baseline contact rate of susceptibles and infectious individuals (equal to both c_S and c_I), implies that $c_R = (1+\alpha)c_B$. Hence, for flexible shielding the weighted average becomes

$$c_B(S+I) + c_B(1+\alpha)R = c_0 \tag{3}$$

or equivalently

$$c_B(1-R) + c_B(1+\alpha)R = c_0 \tag{4}$$

such that

$$\begin{aligned} c_B &= \frac{c_0}{1-R+R+\alpha R}, & (5)\\ &= \frac{c_0}{1+\alpha R}. & (6) \end{aligned}$$

As a result, the force of infection is proportional to:

$$\frac{c_B^2 I}{c_0} \tag{7}$$

or

$$\frac{c_0 I}{(1+\alpha R)^2}. \tag{8}$$

The resulting SIR dynamics with flexible shielding are:

$$\begin{aligned} \dot{S} &= -\beta \frac{SI}{(1+\alpha R)^2} & (9)\\ \dot{I} &= \beta \frac{SI}{(1+\alpha R)^2} - \gamma I & (10)\\ \dot{R} &= \gamma I. & (11) \end{aligned}$$

Flexible shielding has an even stronger effect on epidemic outbreaks than analysis of the core shielding model ($1/(1+\alpha R)$) presented in the main text (see Extended Data Figure 1). In keeping the number of contacts constant, I and S individuals diminish their interactions given more shields to replace them.

Fixed shielding: In a fixed shielding mechanism, recovered individuals have $1+\alpha$ greater contact rates relative to their original baseline, such that the new weighted average is:

$$c_B(1-R) + c_0(1+\alpha)R = c_0, \tag{12}$$

implying

$$c_B = c_0 \frac{1-(1+\alpha)R}{1-R}. \tag{13}$$

Hence, the force of infection is proportional to:

$$\frac{c_B^2 I}{c_0} \tag{14}$$

or

$$\frac{c_0 \left(1-(1+\alpha)R\right)^2}{(1-R)^2} I. \tag{15}$$

The resulting SIR dynamics with fixed shielding are:

$$\dot{S} = -\beta \frac{SI\left(1-(1+\alpha)R\right)^2}{(1-R)^2} \tag{16}$$

$$\dot{I} = \beta \frac{SI\left(1-(1+\alpha)R\right)^2}{(1-R)^2} - \gamma I \tag{17}$$

$$\dot{R} = \gamma I. \tag{18}$$

This model is applicable insofar $(1+\alpha)R \leq 1$, such that the epidemic must have outbreak size $R_\infty \leq 1/(1+\alpha)$. Like flexible shielding, the fixed shielding mechanism also outperforms the core shielding model presented in the main text (see Extended Data Figure 1).

Assumptions for Age-Structured Model

We present the age-structured epidemiological model discussed in the main text. Consider a population of susceptible S, exposed E, infectious asymptomatic I_{asym}, infectious symptomatic I_{sym}, and recovered R who are free to move, without restrictions in a 'business as usual' scenario. A subset of symptomatic cases will require hospital care, which we further divide into subacute I_{hsub}, and critical/acute (i.e., requiring ICU intervention) I_{hcrit} cases. Vital dynamics (births and other causes of death) are ignored for simplicity. The model is visually represented in Extended Data Figure 2 and the system of nonlinear differential equations governing this age-structured epidemiological model are shown below:

$$\frac{dS(a)}{dt} = -\overbrace{\frac{\beta_s S(a) I_{sym,tot}}{N_{tot} + \alpha R_{Shields}}}^{symptomatic\ contact} - \overbrace{\frac{\beta_{asym} S(a) I_{asym,tot}}{N_{tot} + \alpha R_{Shields}}}^{asymptomatic\ contact}$$

$$\frac{dE(a)}{dt} = \overbrace{\frac{\beta_{sym} S(a) I_{sym,tot}}{N_{tot} + \alpha R_{Shields}}}^{symptomatic\ contact} + \overbrace{\frac{\beta_{asym} S(a) I_{asym,tot}}{N_{tot} + \alpha R_{Shields}}}^{asymptomatic\ contact} - \overbrace{\gamma_e E(a)}^{onset\ of\ infectiousness}$$

$$\frac{dI_{asym}(a)}{dt} = \overbrace{p(a)\gamma_e E(a)}^{asymptomatic\ onset} - \overbrace{\gamma_a I_{asym}(a)}^{recovery}$$

$$\frac{dI_{sym}(a)}{dt} = \overbrace{(1-p(a))\gamma_e E(a)}^{symptomatic\ onset} - \overbrace{\gamma_s I_{sym}(a)}^{transfer\ from\ I_{sym}}$$

$$\frac{dI_{hsub}(a)}{dt} = \overbrace{h(a)(1-\xi(a))\gamma_s I_{sym}(a)}^{subcritical\ cases} - \overbrace{\gamma_h I_{hsub}(a)}^{transfer\ from\ I_{hsub}}$$

$$\frac{dI_{hcrit}(a)}{dt} = \overbrace{h(a)\xi(a)\gamma_s I_{sym}(a)}^{critical\ (ICU)\ cases} - \overbrace{\gamma_h I_{hcrit}(a)}^{transfer\ from\ I_{hcrit}}$$

$$\frac{dR(a)}{dt} = \overbrace{\gamma_a I_{asym}(a)}^{recovery\ from\ I_{asym}} - \overbrace{(1-h(a))\gamma_s I_{sym}(a)}^{recovery\ from\ I_{sym}} - \overbrace{\gamma_h I_{hsub}(a)}^{recovery\ from\ I_{hsub}} - \overbrace{(1-\mu)\gamma_h I_{hcrit}(a)}^{recovery\ from\ I_{hcrit}}$$

$$\frac{dD(a)}{dt} = \overbrace{\mu\gamma_h I_{hcrit}(a)}^{mortality},$$

where $I_{sym,tot}$ are the total number (across all age classes) of symptomatic infectious individuals, $I_{asym,tot}$ are the total number of asymptomatic infectious individuals, N_{tot} is the total number of alive individuals (not in the D state), and $R_{Shields}$ are the number of recovered individuals who could serve as serological shields - which we define as those of ages between 20 and 59. The assumed model parameters used in the baseline models are shown in Tables S1 and S2 [40].

Varying the intensity of the outbreak $\mathcal{R}_0$

Based on the parameters in Tables S1 and S2, $\mathcal{R}_0$ is calculated as a weighted average between the symptomatic and asymptomatic reproduction numbers R_{asym}, respectively R_{sym}:

$$R_0 = pR_{asym} + (1-p)R_{sym}. \tag{19}$$

These can be further expanded based on age groups to obtain:

$$R_0 = \sum_{a \in \text{Age Groups}} p(a) \cdot f(a) \cdot R_{asym}(a) + (1-p(a)) \cdot f(a) \cdot R_{sym}(a). \tag{20}$$

which yields a basic reproduction number of about 1.57 in the low scenario and 2.33 in the high scenario.

Initial conditions in the extended model

The baseline model assumes a population of 10,000,000 with age demographics as given in Table S2 unless stated otherwise. An initial outbreak is seeded in this population given one exposed individual in the 20-29 age class. The simulation is run forward until 10,000 people have been exposed to the virus (i.e. 10,000 people are no longer in the susceptible states) - we use this time point (which we denote time 0 in our simulations) as the time at which intervention policies might be applied. At this point, once 10,000 people have already been exposed we simulate the dynamics forward either with, or without the interventions, described in the main text and below.

Interaction substitution and demography

Demography has potential impacts on the spread and consequences of coronavirus and on the efficacy of intervention strategies. We evaluated the baseline model and shielding scenarios $\alpha = 2$ and $\alpha = 20$ given the age structure for the United States, i.e., including 50 states, Washington D.C., and Puerto Rico. The states include significant variation in the fraction of population over 60, ranging from less than 16% (Utah) to above 28% (Maine). We observe a demographic dependence on efficacy of shielding to both per capita cumulative deaths and per capita peak ICU demand, linked to the fraction of the population that is 60 and above. The relationship is linear under both the low and high $\mathcal{R}_0$ scenarios (see Extended Data Figure 3). Outcomes are better when the population has relatively more younger individuals (given that age stratified risk will favor improved outcomes for those who are infected). However, notably, shielding reduces the difference in outcomes, e.g., whereas the cumulative deaths for Utah are 440 (400) less per 100,000 than Maine in the baseline case they are only 210 (120) less per 100,000 than Maine in the $\alpha = 20$ shielding case for the high (low) $\mathcal{R}_0$ scenarios. Hence, demographic distributions that are relatively older will favor deployment of shields (in a relative sense). We note that although we have treated state level demographics uniformly, this result also points toward the benefits of shield immunity in areas with right-shifted age distributions as potential targets for intervention - and potential consequences for deployment of shields in other countries with right-shifted demographics (e.g., Italy).

Variation with asymptomatic cases

We investigate the impact of asymptomatic transmission on the efficacy of immune shielding as an intervention. First, we fixed the intrinsic asymptomatic fraction p from 0.5 to 0.95 for scenarios corresponding to $\alpha = 0, 2$ and 20 (Extended Data Figure 4). Irrespective of the shielding preference α increases in p reduces total deaths and ICU cases by $\approx 90\%$ when R_0 is constant and more than 90% when R_0 is a function of p, given variation from $p = 0.5$ to $p = 0.95$. We observed that the impact of immune shielding is higher at low p. Second, we consider the effects of age-dependent variation in the intrinsic asymptomatic fraction, $p(a)$, by fixing the average p at 0.5, 0.75 and 0.9, given observations of increasing risk based on clinical outcome data from Wuhan, China [41] (Extended Data Figure 5). The impact of immune shielding is robust to observed age-specific variation p, i.e., leading to significant decreases of projected deaths and ICU cases (Extended Data Figure 6).

Impacts of waning immunity

We extended the core model to account for potential impacts of waning immunity by including explicit state-structured shield compartments consisting of newly recruited recovered individuals (H_1) and late stage recovered individuals that can revert to become susceptible (H_2). In effect, the immunity duration was assumed to be gamma distributed, after which recovered individuals become susceptible. This is a conservative assumption, given that individual who lose immunity are likely to have less severe illness if re-infected (but could still pass on an infection to immunological naive individuals).

Extended Data Figure 7 shows the outbreak dynamics for the high and low R_0 scenarios with an average immunity duration of 2 months. Immune shielding can still significantly reduce the number of deaths and the peak number of ICU beds needed for both scenarios, especially for the strong shielding case ($\alpha = 20$). In Extended Data Figure 8 we systematically explore how the cumulative deaths, maximum ICU beds needed, and total number of cases depend on the immunity duration. The results show that the efficacy of immune shielding is robust to the duration of immunity, insofar as the duration of immunity persists on the order of multiple months (and not multiple weeks).

Optimised age-dependent immune shielding deployment

In the previous sections, we assumed that shields (recovered individuals aged 20-59) were deployed such that they interact with people of all ages equally. In other words, all the susceptible individuals (across ages) have an infection rate that scales with $I_{tot}/(N_{tot}+\alpha R_{shields})$ such that the shields are uniformly interacting with all ages. In this section, we explore the outcome of having the shields act in positions where they could be more or less-likely to interact with different age groups, *i.e.,* using the same effort as in the core model, then taking the $\alpha R_{shields}$ of effort but distributing it non-uniformly across ages. To explore the 'optimised' distributions of the shields effort, we introduce non-uniform shield interactions in the model. To do so, we modify the equations of $S(a)$ and $E(a)$ in the core model as follows:

$$\begin{aligned}\frac{dS(a)}{dt} &= -\beta_a \frac{S(a)I_{asym,tot}}{N_{tot}+\alpha R_{shields}(\theta_a/f_a)} - \beta_s \frac{S(a)I_{sym,tot}}{N_{tot}+\alpha R_{shields}(\theta_a/f_a)} \\ \frac{dE(a)}{dt} &= \beta_a \frac{S(a)I_{asym,tot}}{N_{tot}+\alpha R_{shields}(\theta_a/f_a)} + \beta_s \frac{S(a)I_{sym,tot}}{N_{tot}+\alpha R_{shields}(\theta_a/f_a)} - \gamma_e E(a),\end{aligned} \tag{21}$$

where f_a is the fraction of the population of age a (f_a-s are fixed parameters) and θ_a is the distributed shielding fraction of the sub-population class of age a, i.e. how we distribute the shields to interact across different age classes. θ_a are the optimization variables. In addition, we define the ratio θ_a/f_a as the age-dependent shielding concentration. When $f_a/\theta_a = 1$ for all ages a, the uniform shields interactions case is recovered i.e. we recover the core model. We note that $\sum_a \theta_a = 1$ such that the effort is the same as in the core model, but allowing for asymmetric distribution across ages. For example, if 25% percent of the population belongs to class a and gets all the shields protection, then $f_a = 0.25$ and $\theta_a = 1$, this implies $\theta_a/f_a = 4$, i.e. a 4-fold boosted protection for that particular class.

The optimization objective is to minimize total deaths $D_{tot}(t_f)$, where t_f is the final time of the simulation – 1 year after shielding begins, while keeping ICU beds less than the maximum carrying capacity B at every time instant. We seek to find the optimum distribution for deploying the effort of the serological shields. The non-uniform shielding fraction can be represent by a vector $\Theta = [\theta_1,\ ...,\ \theta_{10}]$, and we aim to solve the following minimization problem:

$$\min\ \mathcal{J}(\Theta) = \int_{t_0}^{t_f} \overbrace{W_i \times d(I^{tot}_{hcri}(t))}^{\text{barrier function (constraint)}}\ dt\ +\ \overbrace{W_d \times D_{tot}(t_f)}^{\text{costs of deaths}}, \tag{22}$$

$$\text{subject to } \sum_{a=1}^{10} \theta_a = 1\ ,\ \theta_a \geq 0 \quad \forall\ a = 1,\ 2,\ ...,\ 10; \tag{23}$$

where W_i are W_d are weight regulators. The barrier function d is chosen such that it increases the cost dramatically as the number of ICU beds in use approach the capacity B of the system, to prevent overloading the healthcare system. To satisfy this property, we pick $d(x) = \log\left(\frac{1}{B-x}\right)$. The barrier function goes to infinity as x approaches B from the left. Here, we consider the maximum capacity B as a 'strict' (or 'hard') constraint and any distributed shielding fraction Θ that leads to the ICU beds exceeding B is not considered a feasible shielding deployment. Given the simulation results shown in main text, we set B as 200 ICU beds per 100,000 for the high scenario case and $B = 80$ ICU beds per 100,000 people for the low scenario case.

The optimization approach allows us to evaluate if it is possible to improve the effectiveness of serological shields, by deploying them unevenly across a population. Moreover, the barrier function in the cost function is negative if $I_{hcri}(t) < B - 1$, which is a 'reward' if occupancy of the ICU beds is low. In practice, we set W_i to be arbitrarily small since it serves much like a constraint, e.g., $W_i = 10^{-7}$. We set $W_d = 1$ as minimizing deaths is the primary goal. The optimization problem (eq. 22) is solved via a *genetic algorithm* [42] using `matlab's` built-in optimization function `ga`, with the maximum generation number (set to 30) serving as the stopping criterion [43].

Extended Data Figure 9 shows that an improved way of distributing shielding effort is as follows: prioritize low, but non-zero, shielding of young and place increasing effort on shielding elderly members of the population (see Extended Data Figure 10 for shielding concentrations). Using the optimized shielding deployment, the reduction in deaths ($D_{tot}(t_f)$) is significant. The results suggest advantages of preferentially shielding those who are most at risk.

Data Availability

Population demographics for US states were obtained from the United States Census Bureau for the year 2018 [44].

Code Availability

All simulation and figure codes used in the creation of this manuscript are available at `https://github.com/WeitzGroup/covid_shield_immunity`. **MATLAB:** The core model; and extensions to consider variation of asymptomatic to symptomatic cases, the impact of dual intervention of social distancing and serological shielding, the effects of waning immunity, and age-dependent deployment of shields were simulated using MATLAB. Model simulations were numerically integrated using ODE45 [45, 46] in MATLAB R2019a. **Julia:** The core model was reproduced

in Julia [47], and extended to look at the affect of different age demographics on disease severity and intervention efficacy. Epidemiological simulations were performed using a 5/4 Runge-Kutta method [48] implemented in the DifferentialEquations.jl package [49]. **R:** The core model was reproduced in R. Simulations were performed in R using the ode45 method [45] in the deSolve package [50].

40 Ferguson, N. *et al.* Impact of non-pharmaceutical interventions (NPIs) to reduce COVID19 mortality and healthcare demand (2020). URL `https://www.imperial.ac.uk/media/imperial-college/medicine/sph/ide/gida-fellowships/Imperial-College-{COVID19}-NPI-modelling-16-03-2020.pdf`.

41 Wu, J. T. *et al.* Estimating clinical severity of COVID-19 from the transmission dynamics in Wuhan, China. *Nature Medicine* 1–5 (2020).

42 Whitley, D. A genetic algorithm tutorial. *Statistics and computing* **4**, 65–85 (1994).

43 The MathWorks, I. *Global Optimization Toolbox*. Natick, Massachusetts, United State (2020). URL `https://www.mathworks.com/products/global-optimization.html`.

44 Bureau, U. Annual estimates of the resident population by single year of age and sex for the United States: April 1, 2010 to July 1, 2017 (2017).

45 Dormand, J. R. & Prince, P. J. A family of embedded Runge-Kutta formulae. *Journal of computational and applied mathematics* **6**, 19–26 (1980).

46 Shampine, L. F. & Reichelt, M. W. The Matlab ODE suite. *SIAM journal on scientific computing* **18**, 1–22 (1997).

47 Bezanson, J., Edelman, A., Karpinski, S. & Shah, V. B. Julia: A fresh approach to numerical computing. *SIAM Review* **59**, 65–98 (2017).

48 Tsitouras, C. Runge–Kutta pairs of order 5 (4) satisfying only the first column simplifying assumption. *Computers & Mathematics with Applications* **62**, 770–775 (2011).

49 Rackauckas, C. & Nie, Q. DifferentialEquations.jl – A Performant and Feature-Rich Ecosystem for Solving Differential Equations in Julia. *Journal of Open Research Software* **5** (2017).

50 Soetaert, K. E., Petzoldt, T. & Setzer, R. W. Solving differential equations in R: package deSolve. *Journal of Statistical Software* **33** (2010).

Acknowledgements

We thank P.S. Dodds, M. Lipsitch, K. Levy, D. Muratore, A. Sanz, and J. Shaman for comments and feedback in initial stages of development and to A. Kraay, B. Lopman, and K. Nelson for discussions on serological testing characteristics as part of ongoing collaborative work. Tweet threads by T. Bedford and N. Christakis were influential in refining initial ideas into the current form. Research effort by JSW and co-authors at the Georgia Institute of Technology was enabled by support from grants from the Simons Foundation (SCOPE Award ID 329108), the Army Research Office (W911NF1910384), National Institutes of Health (1R01AI46592-01), and National Science Foundation (1806606 and 1829636). JD was supported in part by grants from the Canadian Institutes of Health Research and the Natural Sciences and Engineering Research Council of Canada.

Author contributions

J.S.W. designed the study, provided oversight for all aspects of the study, developed the core modeling framework, developed simulation code, analyzed models, and wrote the manuscript. S.J.B., A.R.C, D.D., M.D-M., C-Y.L., G.L., A.M., R.R.-G.,S.S. and C.Z. developed simulation code, extended model simulations, analyzed models, and contributed to writing the manuscript. S-W.P. and J.D. contributed to study design, model development, and writing the manuscript.

Competing interests

J.S.W. has received research support from the NSF, NIH, DoD, Burroughs Wellcome Fund, MathWorks, and Simons Foundation. J.D. has received research support from the Canadian Institutes of Health Research and NSERC of Canada.

Intervention Serology and Interaction Substitution: Exploring the Role of 'Immune Shielding' in Reducing COVID-19 Epidemic Spread
Supplementary Information

Joshua S. Weitz,[1,2,3,*] Stephen J. Beckett,[1] Ashley R. Coenen,[2] David Demory,[1] Marian Dominguez-Mirazo,[4,1] Jonathan Dushoff,[5,6] Chung-Yin Leung,[1,2] Guanlin Li,[4,2] Andreea Magalie,[4,1] Sang Woo Park,[7] Rogelio Rodriguez-Gonzalez,[4,1] Shashwat Shivam,[8] and Conan Zhao[4,1]

[1] *School of Biological Sciences, Georgia Institute of Technology, Atlanta, GA, USA*
[2] *School of Physics, Georgia Institute of Technology, Atlanta, GA, USA*
[3] *Center for Microbial Dynamics and Infection, Georgia Institute of Technology, Atlanta, GA, USA*
[4] *Interdisciplinary Graduate Program in Quantitative Biosciences, Georgia Institute of Technology, Atlanta, GA, USA*
[5] *Department of Biology, McMaster University, Hamilton, ON, Canada*
[6] *DeGroote Institute for Infectious Disease Research, McMaster University, Hamilton, ON, Canada*
[7] *Department of Ecology and Evolutionary Biology, Princeton University, Princeton, NJ, USA*
[8] *School of Electrical and Computer Engineering, Georgia Institute of Technology, Atlanta, GA, USA*

(Dated: April 10, 2020)

*Electronic address: jsweitz@gatech.edu; URL: http://ecotheory.biology.gatech.edu

I. SUPPLEMENTARY TABLES

Parameter	Meaning	Value
β_a	Asymptomatic transmission	0.3/day
β_s	Symptomatic transmission	0.6/day
$1/\gamma_e$	Mean exposed period	4 days
$1/\gamma_a$	Mean asymptomatic period	4 (low) and 6 (high) days
$1/\gamma_s$	Mean symptomatic period	4 (low) and 6 (high) days
$1/\gamma_h$	Mean hospital period	10 days
$\mathcal{R}_0$	Basic reproduction number	1.57 (low) and 2.33 (high)

TABLE S1: Epidemiological characteristics.

Age	Frac. of Population f	Frac. Asymptomatic p	Hospital Frac. h	ICU (given hospitalization) Frac. ξ
0-9	0.12	0.95	0.001	0.05
10-19	0.14	0.95	0.003	0.05
20-29	0.14	0.9	0.012	0.05
30-39	0.13	0.8	0.032	0.05
40-49	0.13	0.7	0.049	0.063
50-59	0.13	0.6	0.102	0.122
60-69	0.10	0.4	0.166	0.274
70-79	0.06	0.2	0.243	0.432
80-89	0.04	0.2	0.273	0.709
90-99	0.01	0.2	0.273	0.709

TABLE S2: Age-stratified risk for COVID-19. Of note, the model assumes that 50% of ICU cases die.

Extended Data 1

Intervention Serology and Interaction Substitution: Exploring the Role of 'Immune Shielding' in Reducing COVID-19 Epidemic Spread

Joshua S. Weitz,[1,2,3,*] Stephen J. Beckett,[1] Ashley R. Coenen,[2] David Demory,[1] Marian Dominguez-Mirazo,[4,1] Jonathan Dushoff,[5,6] Chung-Yin Leung,[1,2] Guanlin Li,[4,2] Andreea Magalie,[4,1] Sang Woo Park,[7] Rogelio Rodriguez-Gonzalez,[4,1] Shashwat Shivam,[8] and Conan Zhao[4,1]

[1] *School of Biological Sciences, Georgia Institute of Technology, Atlanta, GA, USA*
[2] *School of Physics, Georgia Institute of Technology, Atlanta, GA, USA*
[3] *Center for Microbial Dynamics and Infection, Georgia Institute of Technology, Atlanta, GA, USA*
[4] *Interdisciplinary Graduate Program in Quantitative Biosciences, Georgia Institute of Technology, Atlanta, GA, USA*
[5] *Department of Biology, McMaster University, Hamilton, ON, Canada*
[6] *DeGroote Institute for Infectious Disease Research, McMaster University, Hamilton, ON, Canada*
[7] *Department of Ecology and Evolutionary Biology, Princeton University, Princeton, NJ, USA*
[8] *School of Electrical and Computer Engineering, Georgia Institute of Technology, Atlanta, GA, USA*

(Dated: April 10, 2020)

*Electronic address: jsweitz@gatech.edu; URL: http://ecotheory.biology.gatech.edu

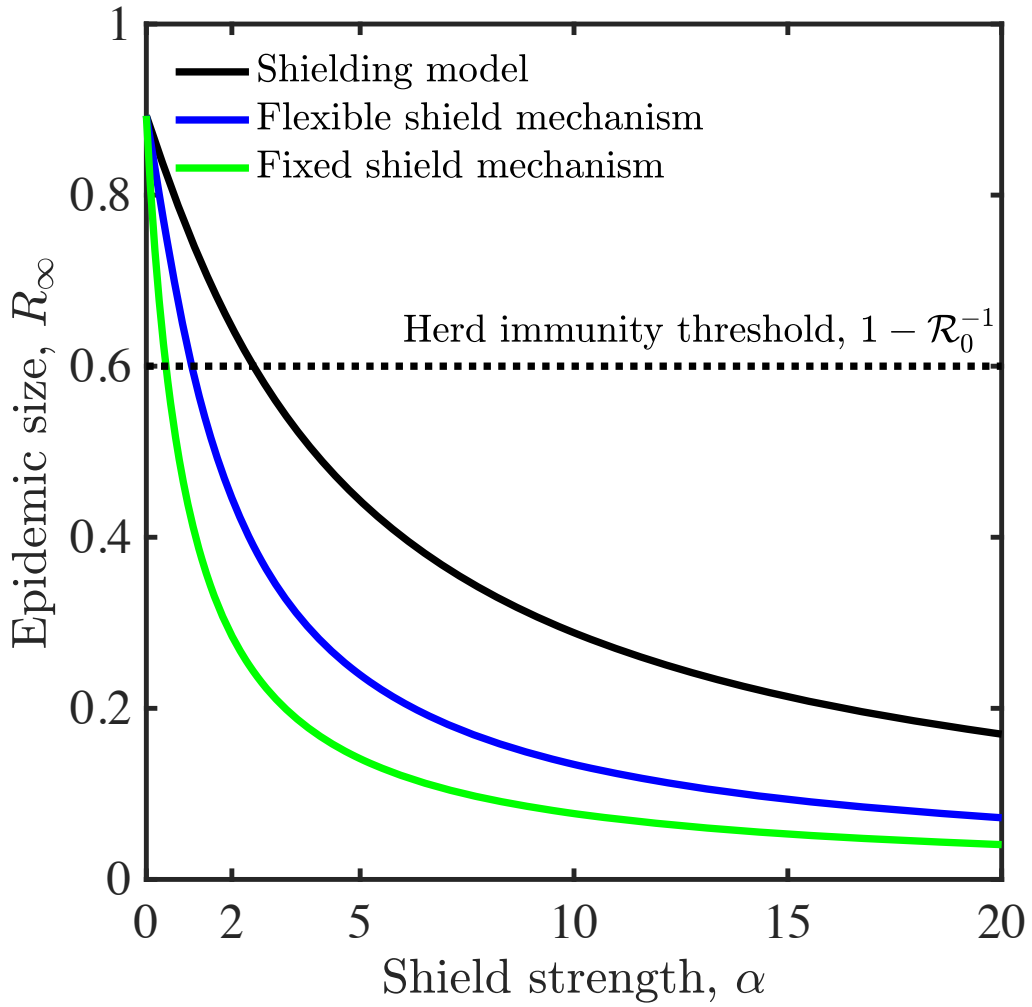

FIG. 1: Impact of shielding mechanisms on final size outcomes in a SIR model. In each case, the epidemic size is plotted (on the y-axis) against the shielding strength, α (x-axis) given $\mathcal{R}_0 = 2.5$. The three curves denote shielding of recovered individuals by a factor of $1 + \alpha$ (black) as described in the main text, a 'flexible' shielding mechanism where the total contact rate is constrained, but recovered individuals vary in their contact rates during the epidemic, and a 'fixed' shielding mechanism where the total contract rate is constrained, but recovered individuals have fixed contact rates during the epidemic. See Methods for details.

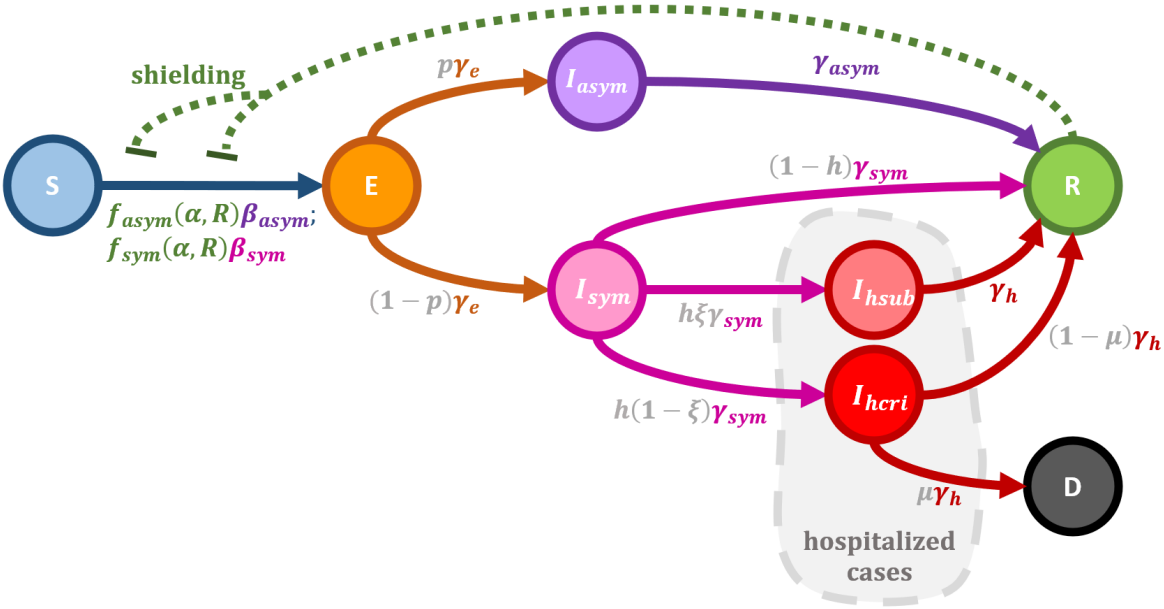

FIG. 2: Model schematic. We consider a population susceptible individuals (S), interacting with infected (I_{sym}, I_{asym}) and recovered (R) individuals. Interactions between susceptible and infectious individuals lead to new exposed cases (E). Exposed individuals undergo a period of latency before disease onset, which are symptomatic (I_{sym}) or asymptomatic (I_{asym}). A subset of symptomatic individuals require hospitalization (I_h) which we further categorize as acute/subcritical (I_{hsub}) and critical (I_{hcri}) cases, the latter of which can be fatal. Individuals who recover can then mitigate the rate of new exposure cases by interaction substitution - what we denote as *immune shielding* - by modulating the rate of susceptible-infectious interactions by $f_{asym}(\alpha, R)$ and $f_{sym}(\alpha, R)$ respectively, where $f_{asym}(\alpha, R) = \frac{S(a)I_{asym,tot}}{N_{tot}+\alpha R_{shields}}$. Here, the *tot* subscript denotes the total number of cases across all ages, i.e. $I_{sym,tot} = \sum_a I_{sym}(a)$.

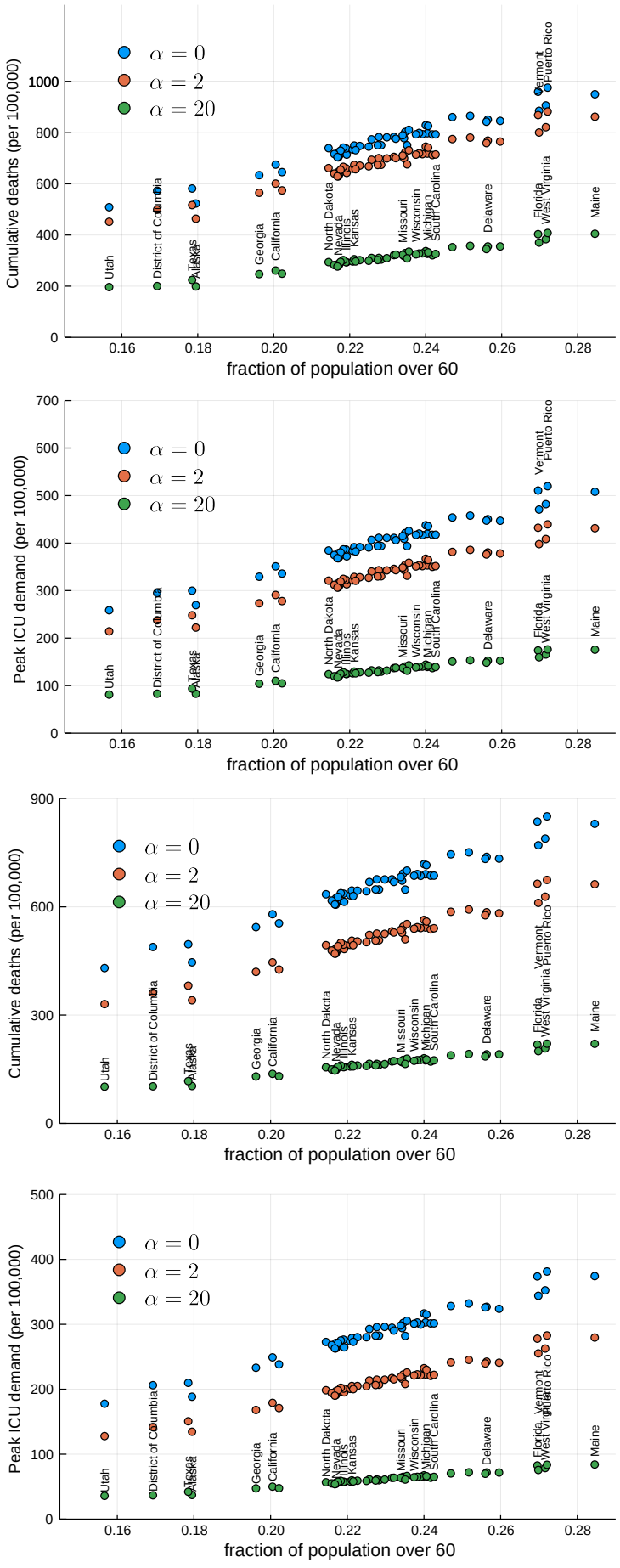

FIG. 3: Impact of demography on the intervention benefits of immune shielding in a high (top two panels) and low (bottom two panels) $\mathcal{R}_0$ scenario. States are ordered by fraction of population above 60 (x-axis) with the baseline, low and high shielding scenarios shown; labels of some but not all states are shown for clarity.

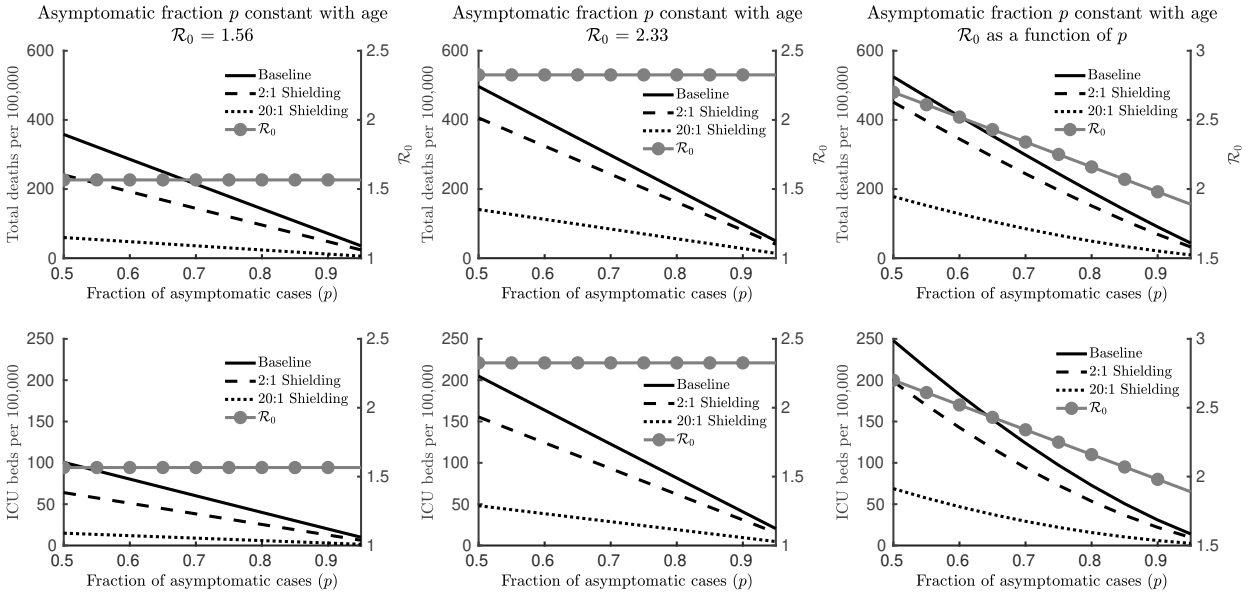

FIG. 4: Impact of p and shielding on the total deaths and the peak ICU cases for a constant R_0 (low scenario left panels, high scenario middle panels) and a dynamic R_0 (right panels). The fraction of asymptomatic p is the same for all ages in the three panels. Shielding offers improvement to outcomes, particularly at lower asymptomatic fractions.

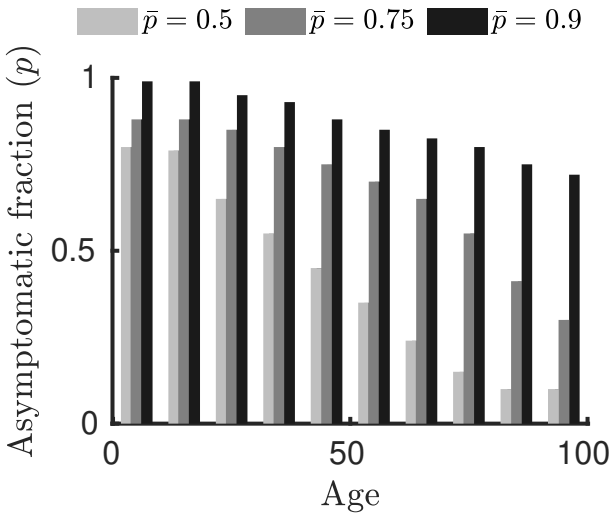

FIG. 5: Age distribution of the asymptomatic fraction p for three different average p: $\bar{p} = 0.5$, $\bar{p} = 0.75$, and $\bar{p} = 0.9$

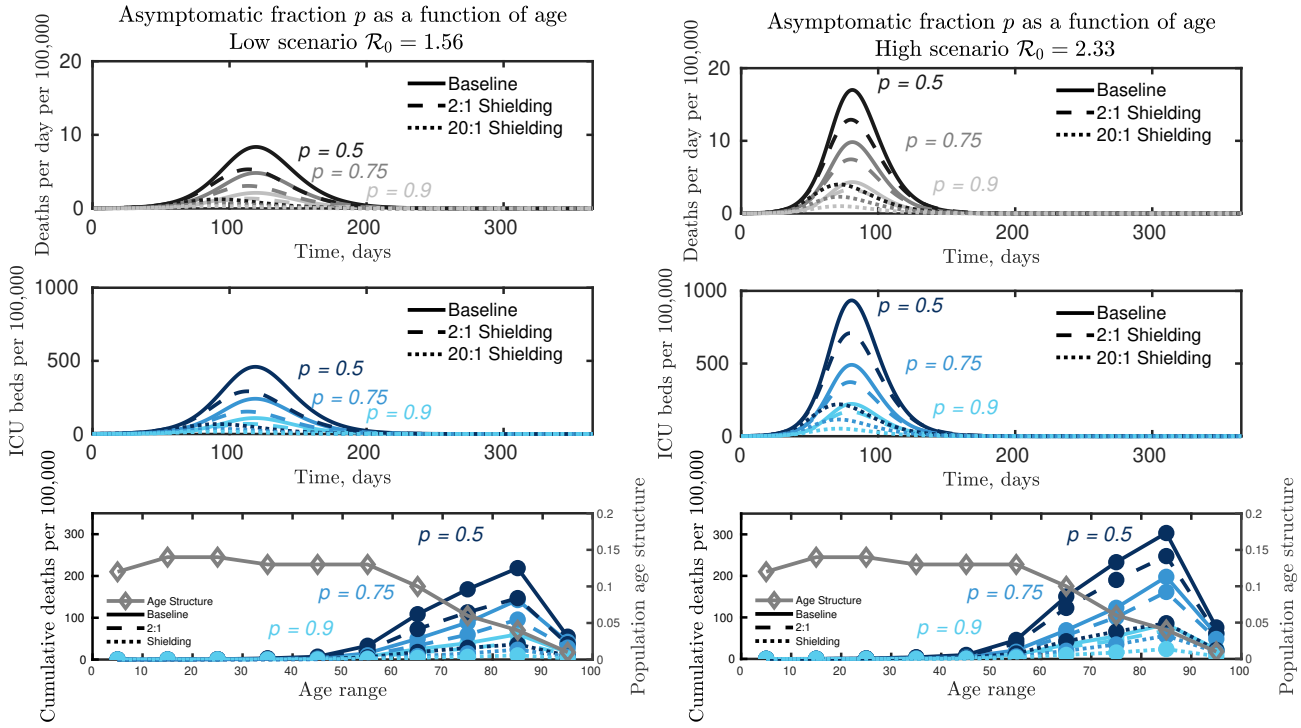

FIG. 6: COVID-19 dynamics in a baseline case without interventions compared to two shielding scenarios ($\alpha = 2$ and $\alpha = 20$) and three age-distributed asymptomatic fraction ($\bar{p} = 0.5$, $\bar{p} = 0.75$ and $\bar{p} = 0.9$) for low scenario ($R_0 = 1.57$ - right panels) and high scenario ($R_0 = 2.33$ - left panels). The impact of immune shielding is robust to observed age-specific variation p, i.e., leading to significant decreases of projected deaths and ICU cases.

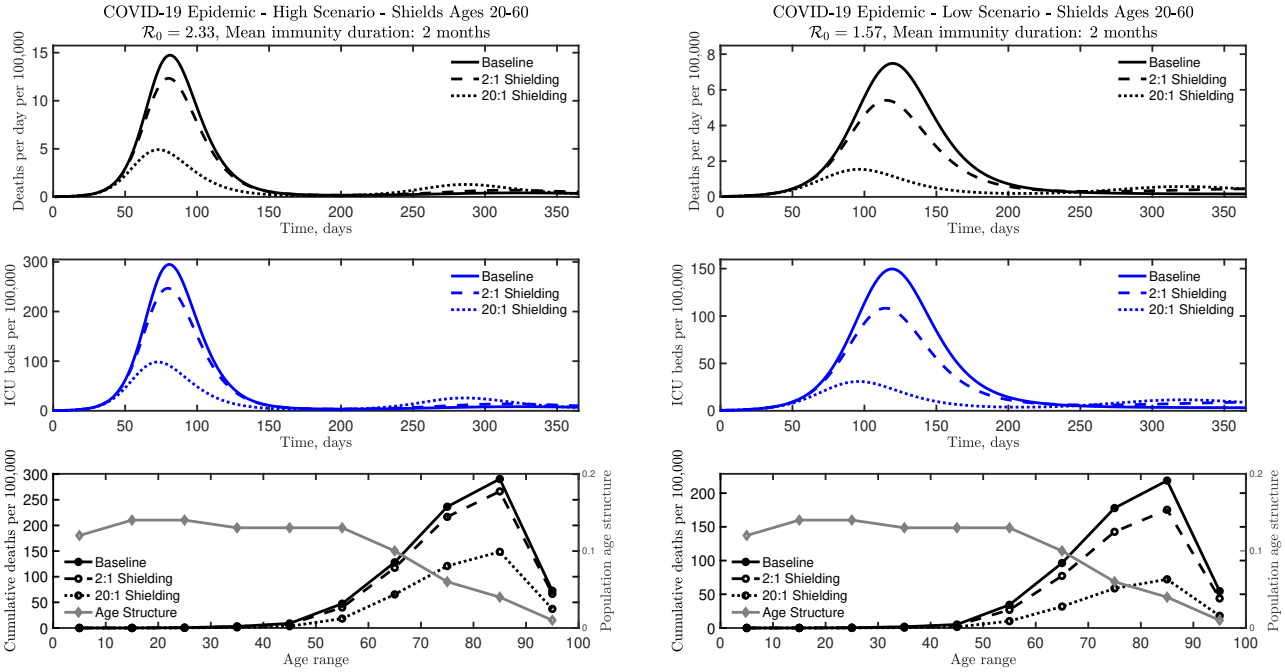

FIG. 7: COVID-19 dynamics for high (left) and low (right) R_0 scenarios. We compared a baseline case without interventions to two shielding scenarios ($\alpha = 2$ and $\alpha = 20$) with a mean immunity duration of 2 months. Immune shielding can still significantly reduce the number of deaths and ICU beds needed for a finite immunity duration.

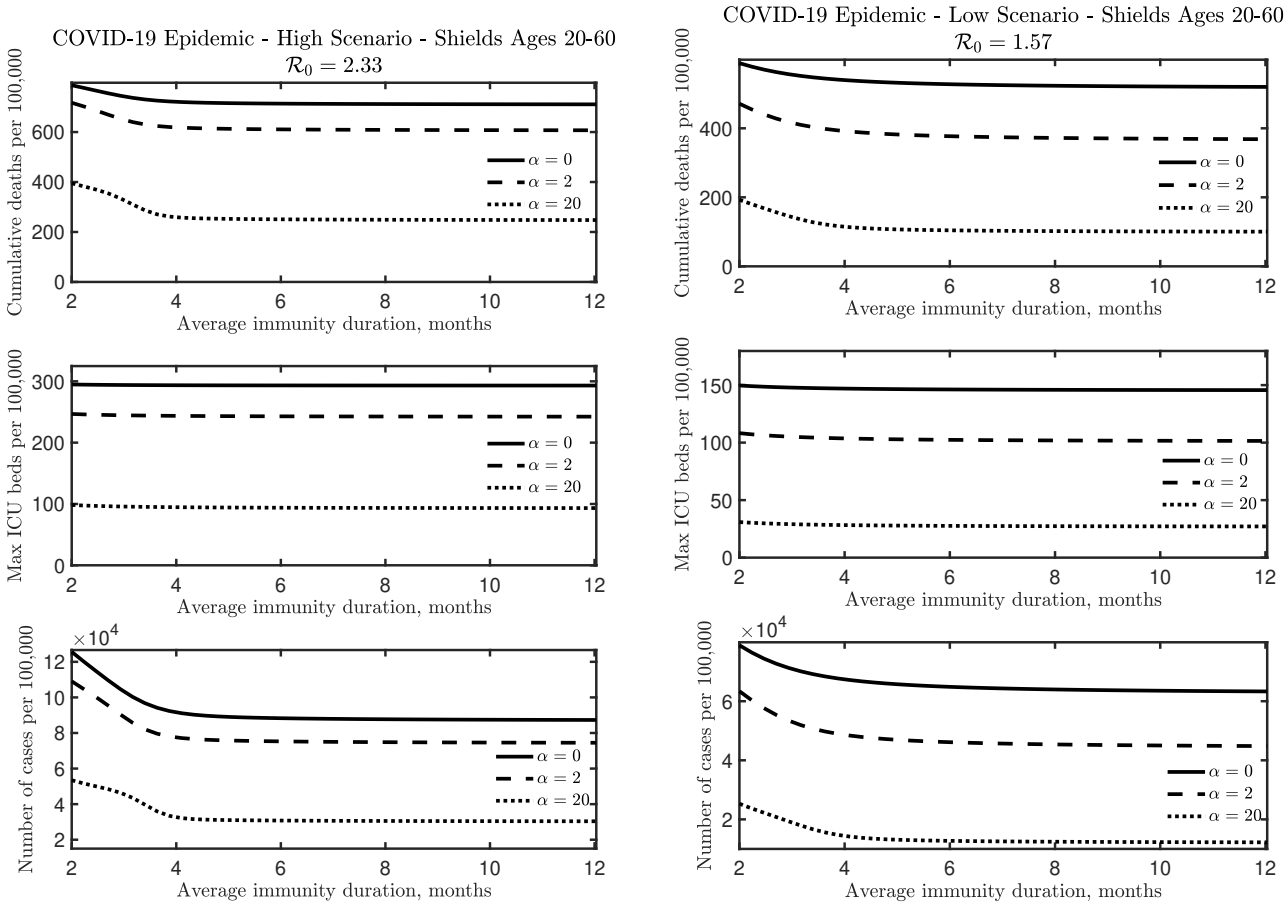

FIG. 8: Comparing the effectiveness of shielding for high (left) and low (right) R_0 scenarios. Shielding is effective at reducing epidemic burden compared to the baseline with no shielding for a wide range of immunity duration. When immunity lasts approximately 4 months or less, re-infection of recovered individuals leads to an increase in the number of deaths and total cases.

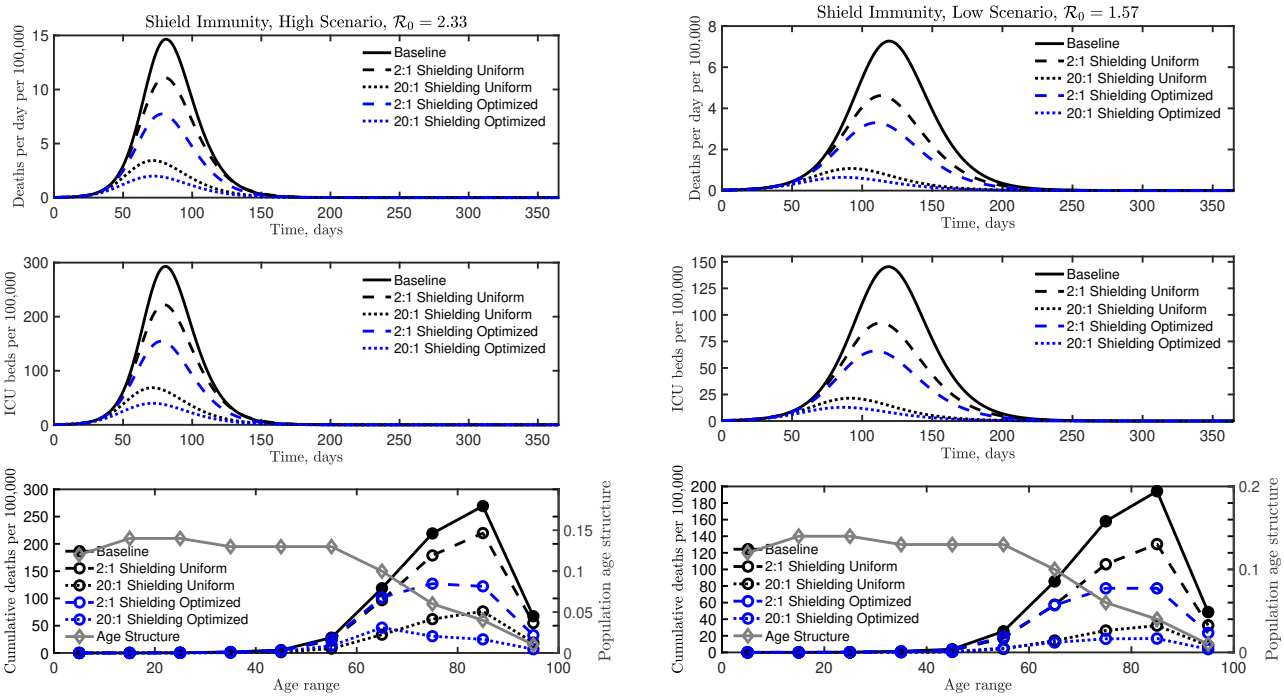

FIG. 9: COVID-19 dynamics in the two shielding scenarios ($\alpha = 2$ and $\alpha = 20$), compared to the scenarios with optimized age dependent shield deployment for the same values of α with the baseline case included for reference. The results are displayed for both high (left) and low (right) R_0 scenarios. The optimal deployment significantly reduces the total death count and the need for ICU beds for both $\alpha = 2$ and $\alpha = 20$.

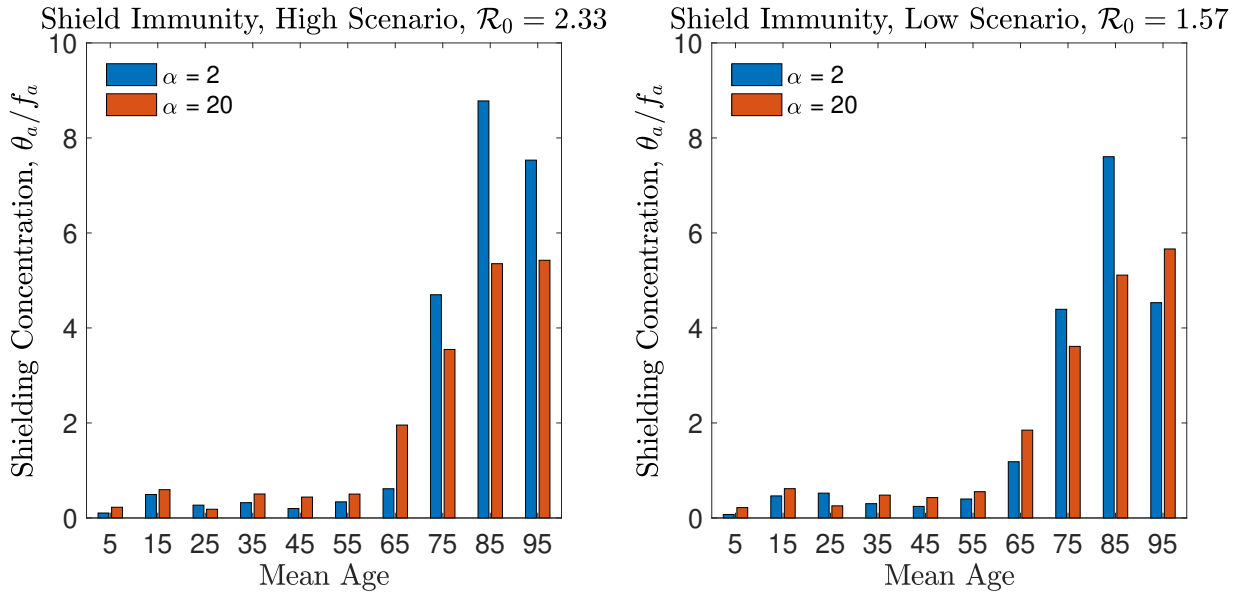

FIG. 10: Optimal shielding concentration for all age classes for high (left) and low (right) $\mathcal{R}_0$ scenarios. The optimal shielding concentrations (for both scenarios) are obtained via solving an optimization problem with low and high shielding levels (see Methods). The optimal shielding concentration (θ_a/f_a) is larger for classes with a higher age, which would reduce casualties as the older population is disproportionately affected by COVID-19.